



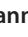
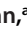







# Septal Class A Penicillin-Binding Protein Activity and $\text{LD}$ -Transpeptidases Mediate Selection of Colistin-Resistant Lipooligosaccharide-Deficient *Acinetobacter baumannii*

 Katie N. Kang,<sup>a</sup>  Misha I. Kazi,<sup>a</sup>  Jacob Biboy,<sup>b</sup>  Joe Gray,<sup>c</sup>  Hannah Bovermann,<sup>a</sup>  Jessie Ausman,<sup>a</sup>  Cara C. Boutte,<sup>a</sup>  
 Waldemar Vollmer,<sup>b</sup>  Joseph M. Boll<sup>a</sup>

<sup>a</sup>Department of Biology, University of Texas Arlington, Arlington, Texas, USA

<sup>b</sup>Centre for Bacterial Cell Biology, Biosciences Institute, Newcastle University, Newcastle upon Tyne, United Kingdom

<sup>c</sup>Biosciences Institute, Newcastle University, Newcastle upon Tyne, United Kingdom

**ABSTRACT** Despite dogma suggesting that lipopolysaccharide/lipooligosaccharide (LOS) was essential for viability of Gram-negative bacteria, several *Acinetobacter baumannii* clinical isolates produced LOS<sup>-</sup> colonies after colistin selection. Inactivation of the conserved class A penicillin-binding protein, PBP1A, was a compensatory mutation that supported isolation of LOS<sup>-</sup> *A. baumannii*, but the impact of PBP1A mutation was not characterized. Here, we show that the absence of PBP1A causes septation defects and that these, together with  $\text{LD}$ -transpeptidase activity, support isolation of LOS<sup>-</sup> *A. baumannii*. PBP1A contributes to proper cell division in *A. baumannii*, and its absence induced cell chaining. Only isolates producing three or more septa supported selection of colistin-resistant LOS<sup>-</sup> *A. baumannii*. PBP1A was enriched at the midcell, where the divisome complex facilitates daughter cell formation, and its localization was dependent on glycosyltransferase activity. Transposon mutagenesis showed that genes encoding two putative  $\text{LD}$ -transpeptidases (LdtJ and LdtK) became essential in the PBP1A mutant. Both LdtJ and LdtK were required for selection of LOS<sup>-</sup> *A. baumannii*, but each had distinct enzymatic activities in the cell. Together, these findings demonstrate that defects in PBP1A glycosyltransferase activity and  $\text{LD}$ -transpeptidase activity remodel the cell envelope to support selection of colistin-resistant LOS<sup>-</sup> *A. baumannii*.

**IMPORTANCE** The increasing prevalence of antibiotic treatment failure associated with Gram-negative bacterial infections highlights an urgent need to develop new alternative therapeutic strategies. The last-line antimicrobial colistin (polymyxin E) targets the ubiquitous outer membrane lipopolysaccharide (LPS)/LOS membrane anchor, lipid A, which is essential for viability of most diderms. However, several LOS<sup>-</sup> *Acinetobacter baumannii* clinical isolates were recovered after colistin selection, suggesting a conserved resistance mechanism. Here, we characterized a role for penicillin-binding protein 1A in *A. baumannii* septation and intrinsic  $\beta$ -lactam susceptibility. We also showed that defects in PBP1A glycosyltransferase activity and  $\text{LD}$ -transpeptidase activity support isolation of colistin-resistant LOS<sup>-</sup> *A. baumannii*.

**KEYWORDS** penicillin-binding protein 1A,  $\text{LD}$ -transpeptidase, peptidoglycan, lipooligosaccharide, Gram-negative, *Acinetobacter*, septation

The Gram-negative cell envelope is tripartite with an inner (cytoplasmic) membrane, a periplasm that includes a thin peptidoglycan layer, and an outer membrane, which is enriched with surface-exposed lipopolysaccharide (LPS) or lipooligosaccharide (LOS). The cell envelope maintains cell shape (1, 2), supports the mechanical load caused by the turgor (3), and enables the cell to rapidly adapt to environmental

**Citation** Kang KN, Kazi MI, Biboy J, Gray J, Bovermann H, Ausman J, Boutte CC, Vollmer W, Boll JM. 2021. Septal class A penicillin-binding protein activity and  $\text{LD}$ -transpeptidases mediate selection of colistin-resistant lipooligosaccharide-deficient *Acinetobacter baumannii*. *mBio* 12:e02185-20. <https://doi.org/10.1128/mBio.02185-20>.

**Editor** Vanessa Sperandio, University of Texas Southwestern Medical Center Dallas

**Copyright** © 2021 Kang et al. This is an open-access article distributed under the terms of the [Creative Commons Attribution 4.0 International license](https://creativecommons.org/licenses/by/4.0/).

Address correspondence to Joseph M. Boll, joseph.boll@uta.edu.

**Received** 7 August 2020

**Accepted** 9 November 2020

**Published** 5 January 2021

challenges. Specialized macromolecular complexes span the cell envelope and coordinate peptidoglycan biosynthesis and LPS/LOS localization.

LPS/LOS is assembled at the inner membrane (4–6) and transported to the outer membrane via LptA-G, which bridges the periplasm and peptidoglycan cell wall (7–12). LPS/LOS glycolipids are based on a highly conserved lipid A moiety that anchors them on the surface-exposed face of the outer membrane. LPS/LOS disruption leads to rapid lysis and death; therefore, it has been targeted with antimicrobials (13). For example, colistin (polymyxin E) is a last-resort antimicrobial used to treat multidrug-resistant bacteria, including the ESKAPE pathogen *Acinetobacter baumannii* (14, 15). Colistin binds the lipid A phosphate groups to perturb the outer membrane barrier, which rapidly kills the bacterium (16, 17). Surprisingly, several *A. baumannii* clinical isolates inactivate LOS biosynthesis and rapidly establish resistance to otherwise toxic colistin concentrations (18, 19). However, certain *A. baumannii* clinical isolates could not develop such resistance. Previous work showed that inactivation of penicillin-binding protein 1A (PBP1A) (encoded by *mrcA*) is a compensatory mutation that supports selection of colistin-resistant LOS<sup>-</sup> *A. baumannii* (19), but the role of PBP1A in *A. baumannii* physiology and how PBP1A mutation alters the cell envelope have not been reported.

In *Escherichia coli*, PBP1A and PBP1B (encoded by *mrcB*) are semi-redundant class A penicillin-binding proteins (aPBPs). aPBPs are bifunctional enzymes, catalyzing both polymerization of glycans via glycosyltransferase (GTase) activity and cross-linking of stem peptides by DD-transpeptidase (DD-TPase) activity. The DD-TPase activity of aPBPs depends on ongoing GTase reactions (20), and in *E. coli* aPBP activity contributes to a substantial amount of the peptidoglycan synthesized per generation (21). PBP1B not only contributes to peptidoglycan maintenance (22) but also interacts with the divisome complex (23, 24), which forms the septum and constricts the cell envelope at the midcell (23, 25). PBP1A interacts with PBP2, which suggests it has a role in cell elongation during growth (26). While PBP1A and PBP1B have distinct roles in growth, only one enzyme is required for growth because the other can compensate (26–28). Specifically, in the absence of PBP1B, PBP1A was enriched at the midcell (26), which implies PBP1A compensates to rescue cell division defects.

In *E. coli*, the majority of transpeptidation reactions in peptidoglycan are catalyzed by PBPs to result in 4-3 cross-links. However, LD-transpeptidases (LD-TPases) such as LdtD, LdtE, and LdtF form 3-3 cross-links (29–31). 3-3 cross-linking becomes essential for *E. coli* survival when LPS transport or biosynthesis is disrupted, presumably because LdtDEF repair peptidoglycan defects together with the GTase function of PBP1B and the DD-carboxypeptidase PBP6a (29). In contrast, LdtA, LdtB, and LdtC attach the outer membrane-anchored Braun's lipoprotein (Lpp) to peptidoglycan, which stabilizes the cell envelope (32).

*A. baumannii* encodes two aPBPs, PBP1A and PBP1B, and two putative LD-TPases (LdtJ and LdtK), but their roles in growth and division have not been characterized. Here, we show that only multiseptated *A. baumannii* strains can support LOS<sup>-</sup> colony formation. In contrast to *E. coli* (26), *A. baumannii* PBP1A is required for proper cell division and PBP1B is unable to compensate in its absence, which enables PBP1A mutants to assemble multiple septal sites. Specifically, disruption of PBP1A GTase activity produces the septation defect, which is also characteristic of LOS<sup>-</sup> *A. baumannii*. PBP1A-mCherry and PBP1A<sub>S459A</sub>-mCherry (DD-TPase mutant) localize at the midcell during growth, where PBP1A potentially interacts with divisome components to synthesize septal peptidoglycan during division. In contrast, PBP1A<sub>E92Q</sub>-mCherry (GTase mutant) did not localize at the midcell, suggesting GTase activity is required for septal localization. In addition to a role in cell division, the PBP1A mutant was resistant to several  $\beta$ -lactam antibiotics relative to wild type and the PBP1B mutant, indicating PBP1A contributes to intrinsic  $\beta$ -lactam susceptibility. Furthermore, *ldtJ* and *ldtK* gene deletions were synthetically lethal in the  $\Delta mrcA$  mutant and were essential for selection of colistin-resistant LOS<sup>-</sup> *A. baumannii*. LdtJ forms 3-3 cross-links and incorporates D-amino acids onto peptidoglycan stem peptides, while LdtK stabilizes the outer membrane.

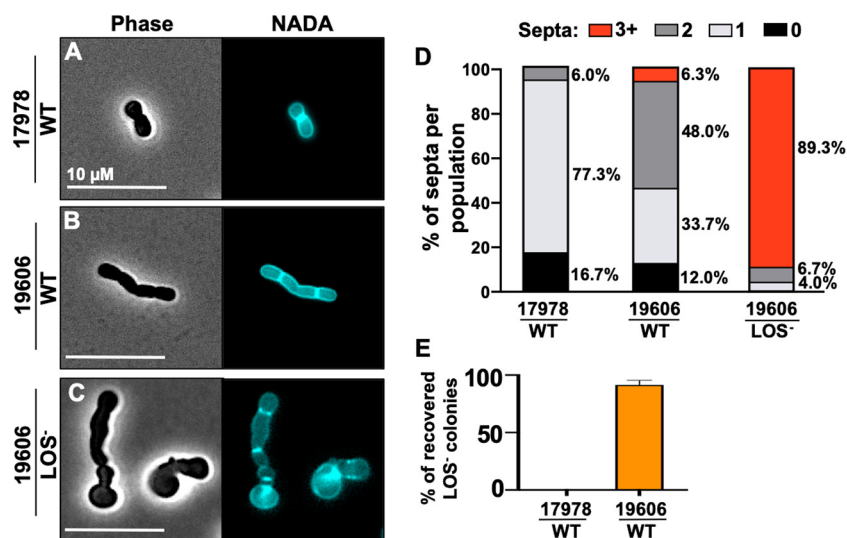


**FIG 1** Microscopy of *A. baumannii* 17978 and 19606 in logarithmic growth phase. (A to C) Phase and fluorescence microscopy of wild-type (WT) 17978 (A), 19606 (reduced levels of PBP1A expression relative to 17978 [19]) (B), and 19606 LOS<sup>-</sup> (C) cells. Cells in mid-logarithmic growth were labeled with NADA. (D) Septa were quantified using ImageJ software ( $n=300$ ) and reported as a percentage of the whole. Data were collected from three experiments, and one representative image and data set were reported. (E) Percentage of LOS<sup>-</sup> *A. baumannii* recovered after colistin selection using  $10^9$  CFU in logarithmic growth phase.

Together, slowed septation, alternative cross-linking, and outer membrane stabilization support colistin selection of LOS<sup>-</sup> *A. baumannii*.

## RESULTS

**Isolation of colistin-resistant LOS<sup>-</sup> *A. baumannii* correlates with defective septation.** We examined *A. baumannii* clinical isolates and found morphological differences between strain ATCC 19606, which produces LOS<sup>-</sup> populations after colistin selection, and strain ATCC 17978, which cannot (19). Cells in logarithmic growth phase were treated with a fluorescent derivative of D-alanine (NADA) (33), which is incorporated into the peptidoglycan cell wall by PBPs and LD-TPases (34–37). Wild-type 17978 cells were coccobacilli with septal assembly localized at the midcell (Fig. 1A), where septal peptidoglycan synthesis produced two daughter cells during division. In contrast, wild-type 19606 bacteria, which demonstrated an 80-fold reduction in PBP1A expression during mid-logarithmic growth (19), were bacilli containing multiple septal sites (Fig. 1B). LOS<sup>-</sup> cells derived from 19606 also contained multiple septal sites (Fig. 1C). Unlike 17978, 19606 and LOS<sup>-</sup> subpopulations contained three or more septa (Fig. 1D), indicating a septation defect. Consistent with previous findings (19), 19606 produced LOS<sup>-</sup> colonies after colistin selection, whereas 17978 did not (Fig. 1E and Table 1). The average lengths and widths of 17978, 19606, and 19606 LOS<sup>-</sup> cells were also calculated (Fig. S1A) and showed that wild-type 19606 and 19606-derived LOS<sup>-</sup> *A. baumannii* populations contained subsets of elongated cells.

To determine if the septation defect was conserved among isolates that support LOS deficiency-mediated colistin resistance, we analyzed several additional *A. baumannii* clinical isolates. Consistent with strain 19606, Ab 5075 (Fig. S1C) and Ab AYE (Fig. S1D) also produced multiseptated bacilli and yielded LOS<sup>-</sup> colistin-resistant isolates (Fig. S1B). In contrast, Ab ACICU (Fig. S1E) and Ab SDF (Fig. S1F) assembled a single septum at the midcell. As with 17978, we could not recover LOS<sup>-</sup> isolates from either ACICU or SDF parent strains (Table 1 and Fig. S1B). Septal quantification showed that Ab 5075 and Ab AYE had subpopulations that produced three or more septa, while Ab ACICU and Ab SDF did not (Fig. S1G). The average length and width of each clinical

**TABLE 1** *A. baumannii* develops colistin resistance through inactivation of lipooligosaccharide (LOS) biosynthesis

<i>A. baumannii</i> strain	Recovery frequency of LOS <sup>-</sup> <i>A. baumannii</i>
Logarithmic growth phase	
<i>Ab</i> 5075	2.33E-08
<i>Ab</i> 5075 $\Delta$ <i>ldtJ</i> ::Tn	N/A <sup>a</sup>
<i>Ab</i> 5075 $\Delta$ <i>ldtK</i> ::Tn	N/A
<i>Ab</i> ACICU	N/A
<i>Ab</i> AYE	8.09E-08
<i>Ab</i> SDF	N/A
ATCC 17978	N/A
ATCC 17978 $\Delta$ <i>mrcA</i>	9.19E-08
ATCC 17978 $\Delta$ <i>mrcA</i> /pPBP1A	N/A
ATCC 17978 $\Delta$ <i>mrcA</i> /pPBP1A <sub>S459A</sub>	N/A
ATCC 17978 $\Delta$ <i>mrcA</i> /pPBP1A <sub>E92Q</sub>	9.19E-08
ATCC 17978 $\Delta$ <i>mrcB</i>	N/A
ATCC 19606	1.47E-07
ATCC 19606 $\Delta$ <i>ldtJ</i>	N/A
ATCC 19606 $\Delta$ <i>ldtJ</i> /pLdtJ	8.99E-06
ATCC 19606 $\Delta$ <i>ldtK</i>	N/A
ATCC 19606 $\Delta$ <i>ldtK</i> /pLdtK	2.11E-07
Stationary phase	
<i>Ab</i> 5075	1.93E-07
<i>Ab</i> ACICU	N/A
<i>Ab</i> AYE	9.59E-07
<i>Ab</i> SDF	N/A
ATCC 17978	N/A
ATCC 17978 $\Delta$ <i>mrcA</i>	1.06E-08
ATCC 17978 $\Delta$ <i>mrcA</i> /pPBP1A	N/A
ATCC 17978 $\Delta$ <i>mrcA</i> /pPBP1A <sub>S459A</sub>	N/A
ATCC 17978 $\Delta$ <i>mrcA</i> /pPBP1A <sub>E92Q</sub>	2.01E-08
ATCC 17978 $\Delta$ <i>mrcB</i>	N/A
ATCC 17978 + 8 g/liter amoxicillin	N/A
ATCC 17978 + 64 g/liter ampicillin	N/A
ATCC 17978 + 4 g/liter carbenicillin	N/A
ATCC 17978 + 32 g/liter mecillinam	N/A
ATCC 17978 + 16 g/liter mezlocillin	N/A
ATCC 17978 + 256 g/liter cefoxitin	N/A
ATCC 17978 + 64 g/liter cefoperazone	N/A
ATCC 17978 + 8 g/liter cefotaxime	N/A
ATCC 17978 + 8 g/liter aztreonam	N/A
ATCC 17978 + 8 g/liter moenomycin	N/A
ATCC 19606	2.13E-07

<sup>a</sup>N/A indicates that no LOS<sup>-</sup> isolates were recovered.

isolate were reported (Fig. S1H). Strains showing three or more septa also produced elongated cell subpopulations.

To determine if elongated morphologies were consistent in growth phases, we also analyzed stationary-phase cultures. Only 19606 (Fig. S2A), 5075 (Fig. S2B), and AYE (Fig. S2C) formed filaments and yielded colistin-resistant LOS<sup>-</sup> isolates in stationary phase (Table 1 and Fig. S2G). 17978 (Fig. S2D), ACICU (Fig. S2E), and SDF (Fig. S2F) maintained a coccobacillus morphology and failed to produce a single LOS<sup>-</sup> isolate after colistin selection (Table 1 and Fig. S2G). The length and width of each isolate in stationary phase were calculated (Fig. S2H). Strains 19606, *Ab* 5075, and *Ab* SDF were elongated relative to 17978, *Ab* ACICU, and *Ab* AYE. While it was previously shown that only select strains supported isolation of LOS<sup>-</sup> *A. baumannii* after colistin selection (19), here we show a correlation between strains with defective septation and selection of colistin-resistant LOS<sup>-</sup> isolates.

**PBP1A mutation induced septal defects and supported isolation of colistin-resistant LOS<sup>-</sup> *A. baumannii*.** Inactivation of the gene encoding PBP1A,  $\Delta$ *mrcA*, is a compensatory mutation that enables colistin selection of LOS<sup>-</sup> 17978 (19). Relative to

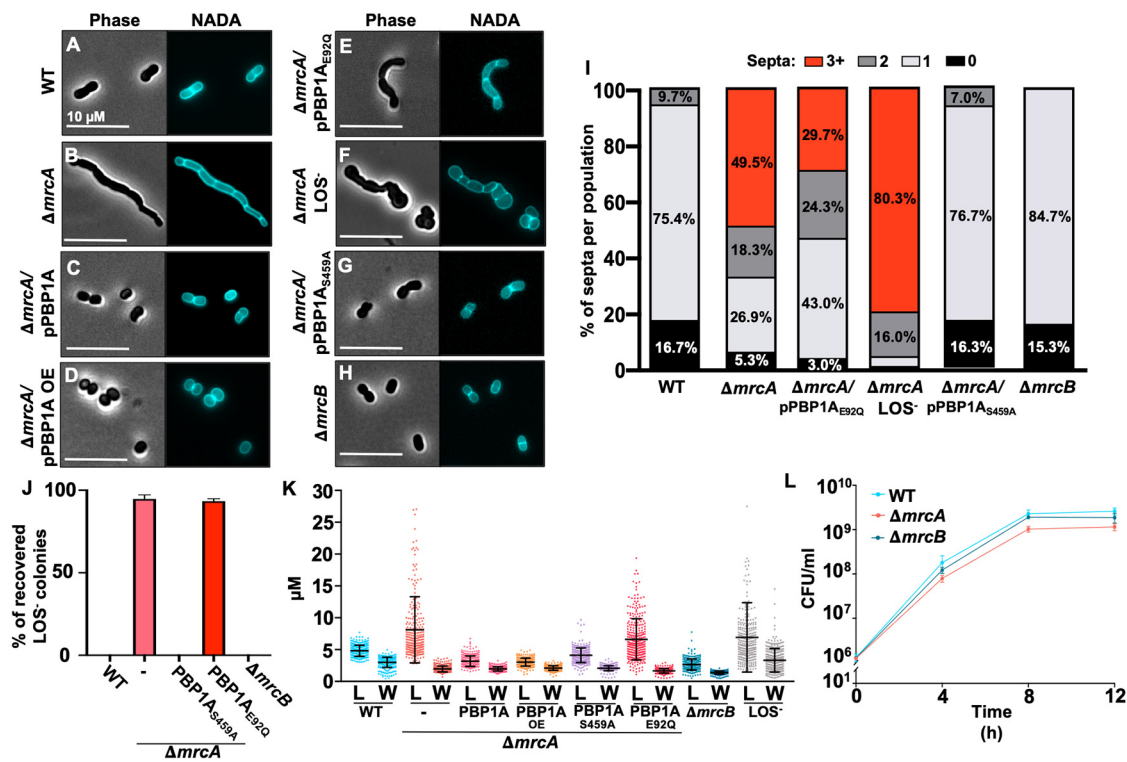


**FIG 2** Microscopy of *A. baumannii* strain 17978 mutants in logarithmic growth phase. (A to H) Phase and fluorescence microscopy of NADA-treated wild-type (WT) (A),  $\Delta mrcA$  (B),  $\Delta mrcA/pPBP1A$  (C),  $\Delta mrcA/pPBP1A$  OE (overexpression) (D),  $\Delta mrcA/pPBP1A_{E92Q}$  (E),  $\Delta mrcA$  LOS<sup>-</sup> (F),  $\Delta mrcA/pPBP1A_{S459A}$  (G), and  $\Delta mrcB$  (H) cells. (I) Septa were quantified using ImageJ software ( $n = 300$ ) and reported as a percentage of the whole. Each experiment was independently replicated three times, and one representative data set was reported. (J) Percentage of recovered LOS<sup>-</sup> *A. baumannii* after colistin selection using  $10^9$  CFU in logarithmic growth phase. (K) Quantification of length (L) and width (W) of each cell population ( $n = 300$ ) was calculated using ImageJ software. Each experiment was independently replicated three times, and one representative data set was reported. Each dot on the graph represents one cell. (L) CFU/ml of wild type and aPBP mutants in rich medium at 37°C.

wild type and two complementation strains with different promoter constructs, the 17978  $\Delta mrcA$  mutant produced multiseptated cell populations in mid-logarithmic growth phase (Fig. 2A to D), resembling 19606, 5075, and AYE morphotypes. Consistent with previous analysis showing that PBP1A GTase activity inhibited colistin selection of LOS<sup>-</sup> colonies (19),  $\Delta mrcA/pPBP1A_{E92Q}$  also produced elongated multiseptated cells (Fig. 2E), similarly to  $\Delta mrcA$  LOS<sup>-</sup> cells (Fig. 2F). In contrast, point mutation of S459A, a residue essential for PBP1A DD-TPase activity (Fig. 2G), and  $\Delta mrcB$  (encoding PBP1B) (Fig. 2H) produced septal patterns indistinguishable from wild-type 17978, ACICU, and SDF. Only PBP1A mutations that induced three or more septal sites (i.e.,  $\Delta mrcA$  and  $\Delta mrcA/pPBP1A_{E92Q}$ ) (Fig. 2I) were sufficient to produce colistin-resistant LOS<sup>-</sup> isolates (Fig. 2J and Table 1). We also measured the lengths and widths of each mutant (Fig. 2K). Only strains with cell populations containing three or more septal sites were elongated. Relative to wild type, the  $\Delta mrcA$  mutant had a growth defect in logarithmic phase (Fig. 2L) when grown in Luria broth at 37°C. The doubling time was  $33.76 \pm 3.7$  and  $36.44 \pm 1.9$  min in wild-type and  $\Delta mrcB$  strains, respectively, whereas the  $\Delta mrcA$  strain had a slightly slower doubling time of  $40.05 \pm 2.6$  min in logarithmic growth phase.

Unlike wild-type 17978,  $\Delta mrcA/pPBP1A_{S459A}$  and  $\Delta mrcB$  strains (Fig. S3A to C),  $\Delta mrcA$  and  $\Delta mrcA/pPBP1A_{E92Q}$  strains demonstrated a filamentous morphology in stationary phase (Fig. S3D and E) that resembled the  $\Delta mrcA$  LOS<sup>-</sup> strain (Fig. S3F) and supported recovery of LOS<sup>-</sup> colistin-resistant isolates (Table 1 and Fig. S3G). The cell lengths, which indicate defective septation, and widths of stationary-phase cultures



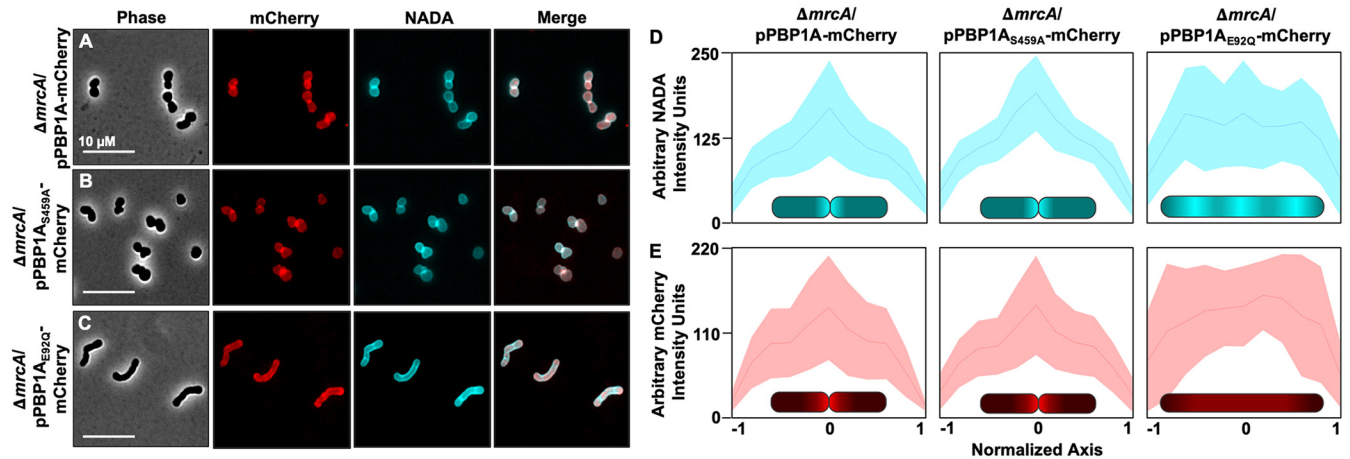


**FIG 3** Localization of PBP1A in *A. baumannii*. (A to C) Phase and fluorescence microscopy of 17978  $\Delta mrcA$  expressing PBP1A (A), PBP1A<sub>S459A</sub> (B), or PBP1A<sub>E92Q</sub> (C) fused to a C-terminal mCherry protein. Cells were labeled with NADA. Merged images are color composites of mCherry and NADA images. (D and E) Localization intensity of NADA (D) and PBP1A-mCherry (E) in cells. Shading indicates standard deviation. Intensity localization graphs generated using ImageJ software with MicrobeJ plugin ( $n=50$ ). Each experiment was independently replicated three times, and one representative data set was reported. Fluorescence localization intensity within cells is illustrated at the bottom.

were measured (Fig. S3H). Consistent with our initial observation that only *A. baumannii* clinical isolates producing cell populations with three or more septal sites support LOS<sup>-</sup> selection, PBP1A mutations that induced multiseptate cell morphotypes also supported LOS<sup>-</sup> isolation. Together, these data indicate that defects in PBP1A-dependent septation correlate with isolation of colistin-resistant LOS<sup>-</sup> *A. baumannii*.

**PBP1A localizes to the division site in *A. baumannii*.** Due to the septation defect in  $\Delta mrcA$  and  $\Delta mrcA$ /pPBP1A<sub>E92Q</sub> strains, we hypothesized that PBP1A contributes to daughter cell formation in *A. baumannii*. To determine PBP1A localization, we fused mCherry to the C terminus of PBP1A (PBP1A-mCherry) and expressed the construct in  $\Delta mrcA$  cells. Expression levels of each PBP1A-mCherry fusion protein in the  $\Delta mrcA$  mutant were equivalent (Fig. S4A), and PBP1A was required for mCherry signal (Fig. S4B). While mCherry fluorescent signal was observed throughout cells when pPBP1A (Fig. 3A) or pPBP1A<sub>S459A</sub> (Fig. 3B) fusion proteins were expressed, increased intensity was evident at the midcell, where the septum forms. These findings indicate that PBP1A localizes at the septal site and potentially interacts with the divisome complex in *A. baumannii*. Phase microscopy showed that pPBP1A-mCherry and pPBP1A<sub>S459A</sub>-mCherry expression fully complemented the  $\Delta mrcA$ -induced division defect to restore the signature *A. baumannii* coccobacillus morphology. In contrast, pPBP1A<sub>E92Q</sub>-mCherry (Fig. 3C) did not localize at the midcell and cells contained multiple septal sites, showing that GTase-defective PBP1A was not sufficient to complement the  $\Delta mrcA$  mutant.

We also treated cells expressing PBP1A-mCherry proteins with NADA, which is incorporated into the peptidoglycan. pPBP1A-mCherry and pPBP1A<sub>S459A</sub>-mCherry colocalized with septal peptidoglycan at the midcell, but pPBP1A<sub>E92Q</sub>-mCherry did not (Fig. 3A to C). To quantify, intensity localization was graphed along the cell axis (Fig. 3D and E). PBP1A and PBP1A<sub>S459A</sub> colocalized with septal peptidoglycan, whereas PBP1A<sub>E92Q</sub> did not. These analyses show not only that the GTase activity of PBP1A is required for proper division in *A. baumannii* but also that GTase activity is required for PBP1A septal site localization.

**Antimicrobial susceptibility in *A. baumannii* aPBP mutants.** To determine the impact of aPBP deletions on antimicrobial susceptibility, MICs were calculated after wild type and the aPBP mutants were treated with several antimicrobials (Table 2). Relative to wild type, the  $\Delta mrcA$  mutant showed increased resistance to all  $\beta$ -lactam antibiotics tested except for carbapenems, which target not only DD-TPases but also LD-TPases (38). These data suggest that PBP1A DD-TPase activity is an intrinsic target that

**TABLE 2** *A. baumannii* MICs

Antimicrobial	MIC (mg/liter) for strain:				
	WT	$\Delta mrcA$	$\Delta mrcB$	$\Delta dtJ$	$\Delta dtK$
$\beta$ -Lactams					
Penicillin derivatives					
Amoxicillin	16.0	>512.0	<8.0	128.0	128.0
Ampicillin	128.0	>1,024.0	128.0	16.0	16.0
Carbenicillin	8.0	>64.0	8.0	4.0	4.0
Mecillinam	64.0	>512.0	64.0	16.0	16.0
Mezlocillin	32.0	>256.0	32.0	128.0	128.0
Cephalosporin derivatives					
Cefoxitin	>512.0	64.0	16.0	128.0	128.0
Cefoperazone	128.0	>512.0	128.0	>512.0	>512.0
Cefotaxime	8.0	32.0	4.0	16.0	8.0
Carbapenems					
Imipenem	0.3	0.3	0.3	<0.01	<0.01
Meropenem	0.1	0.1	0.1	<0.01	<0.01
Monobactam					
Aztreonam	16.0	2.0	2.0	8.0	8.0
Phosphoglycolipid					
Moenomycin	16.0	2.0	2.0	4.0	4.0
Lipopeptide					
Colistin	1.0	1.0	1.0	1.0	1.0
Glycopeptide					
Vancomycin	>512.0	64.0	64.0	64.0	64.0
Metal (mM)					
Copper chloride	5.0	4.5	4.0	3.5	3.0

contributes to  $\beta$ -lactam susceptibility and that PBP1A has a critical role in cross-linking peptidoglycan. However,  $\text{DD-TPase}$  activity is not critical for the function of PBP1A that inhibits formation of LOS<sup>-</sup> cells. Both aPBP mutants showed increased susceptibility to moenomycin, which inhibits GTase activity. No differences in MIC were observed when strains were treated with colistin. Lastly, both aPBP mutants demonstrated increased susceptibility to vancomycin.

**Filamentation is not sufficient for isolation of colistin-resistant LOS<sup>-</sup> *A. baumannii*.** While PBP1A GTase activity is required for proper *A. baumannii* division, defective division is also correlated with isolation of colistin-resistant LOS<sup>-</sup> *A. baumannii*. We next tested if filamentation was sufficient to recover colistin-resistant LOS<sup>-</sup> *A. baumannii*. Previous studies showed that treatment with  $\text{DD-TPase}$ -targeting  $\beta$ -lactams induced filamentation in Gram-negative bacteria (39, 40). Therefore, we treated wild-type 17978 with several  $\beta$ -lactams and moenomycin (Table 2). Wild-type 17978 was grown overnight in 0.5 $\times$  MICs of each antibiotic, and cultures were treated with NADA to visualize morphological changes (Fig. S5A to J). Amoxicillin, cefoperazone, cefotaxime, aztreonam, moenomycin, and cefoxitin treatment induced filamentation (Fig. S5K), likely because they inhibit  $\text{DD-TPase}$  or glycosyltransferase activity required for cell division. In contrast, cells treated with ampicillin, carbenicillin, amdinocillin, and mezlocillin formed spheres (Fig. S5K), suggesting the  $\beta$ -lactams target primarily  $\text{DD-TPases}$  associated with cell elongation. We next performed colistin selection on treated cells to isolate LOS<sup>-</sup> *A. baumannii*; however, we were unable to recover LOS<sup>-</sup> isolates from all treated cultures (Table 1 and Fig. S5L), indicating that filamentation is not sufficient for colistin selection of LOS<sup>-</sup> *A. baumannii*.

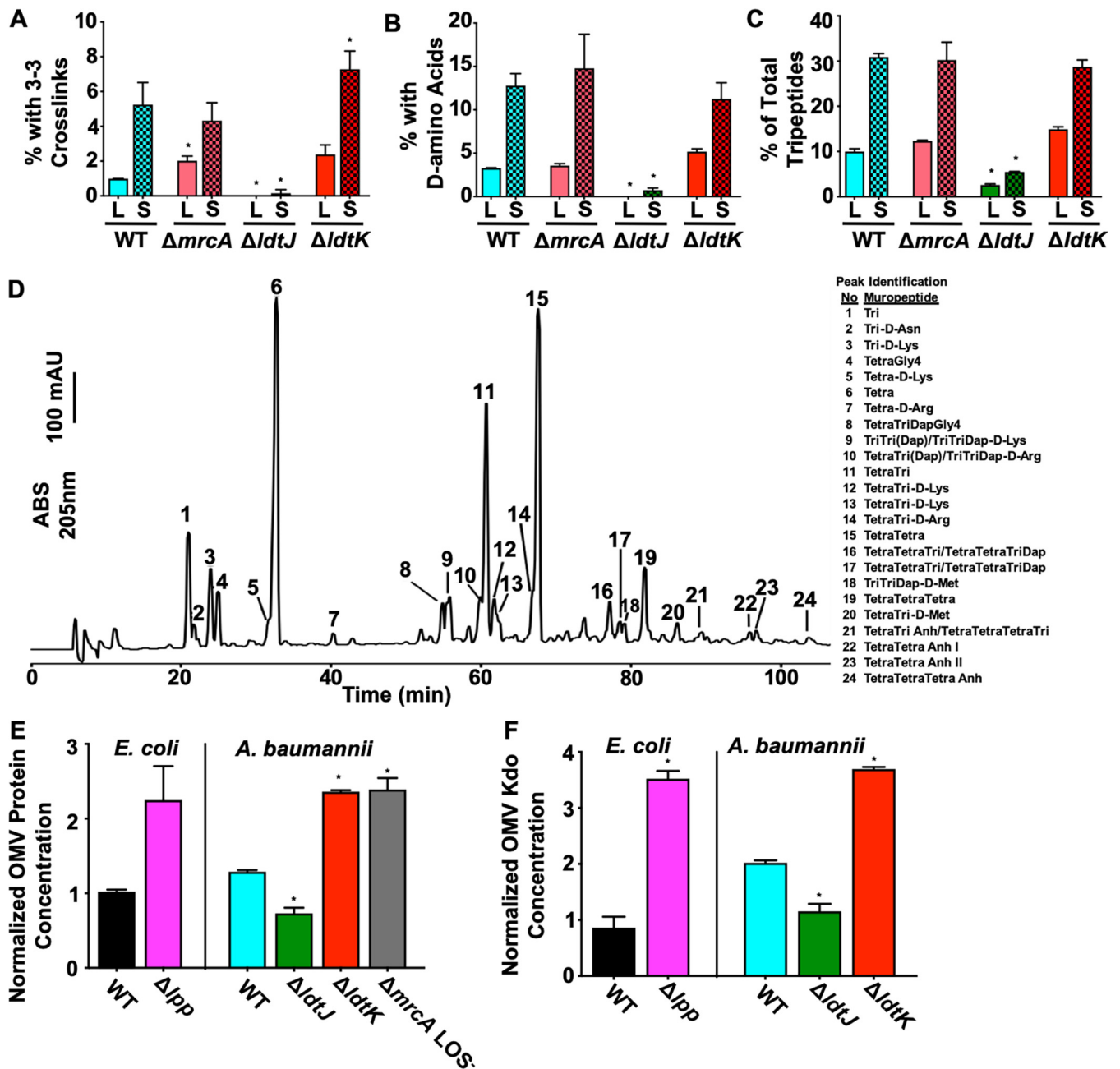


**FIG 4** LD-Transpeptidase activity is required for cell envelope modifications in *A. baumannii*. (A to C) Percentage of total muropeptide content with 3-3 cross-links (A), D-amino acid addition (B), and muropeptide formation (C). L, logarithmic growth phase; S, stationary phase. Error bars indicate variation of two biological replicates. An asterisk indicates significant differences relative to the corresponding wild-type (WT) strain ( $P < 0.05$ ). (D) Chromatogram of the muropeptide content of stationary-phase 17978  $\Delta ldtK$ . The muropeptides are labeled. (E and F) Relative quantification of *E. coli* and *A. baumannii* total protein (E) and Kdo (F) concentrations of outer membrane vesicles (OMVs) in  $\Delta ldtJ$  and  $\Delta ldtK$  strains relative to wild-type (WT) *A. baumannii* and *E. coli*. WT *E. coli* was normalized to 1. Each experiment was independently replicated three times, and one representative data set was reported. Error bars indicate standard deviations. An asterisk indicates significant differences relative to the corresponding WT strain ( $P < 0.05$ ).

**Peptidoglycan modifications resulting from PBP1A mutation.** Since we found that the  $\Delta mrcA$  mutant showed increased resistance against several DD-TPase-targeting  $\beta$ -lactam antibiotics, we next sought to determine if the mutation altered the muropeptide composition in logarithmic and stationary phase. Muropeptide compositions of both wild-type and  $\Delta mrcA$  strains were analyzed (Table S1A) and showed increased peptidoglycan modifications in stationary phase relative to logarithmic growth phase. Specifically, 3-3 cross-linking and incorporation of D-amino acids increased (Fig. 4A and



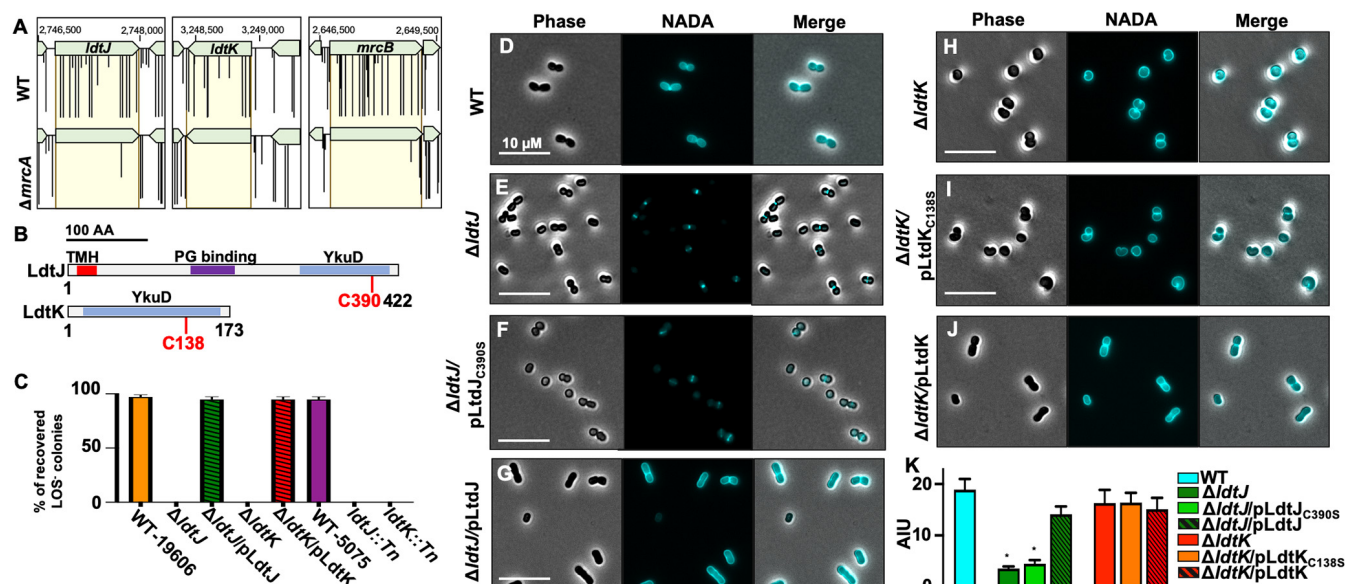


**FIG 5** LD-Transpeptidases are required for isolation of LOS<sup>-</sup> *A. baumannii*. (A) Transposon sequencing analysis of *ldtJ*, *ldtK*, and *mrcB* in wild-type (WT) and  $\Delta mrcA$  17978 *A. baumannii*. Yellow-highlighted areas indicate genes of interest. Black lines indicate transposon insertion sites and abundance. (B) Schematic of domain organization of LdtJ and LdtK. (C) Percentage of recovered LOS<sup>-</sup> colonies after colistin selection of wild-type and mutant 19606 and Ab 5075 strains in logarithmic phase. (D to J) Phase and fluorescence microscopy of NADA-treated wild-type and  $\Delta ldtJ$  (D to G) and  $\Delta ldtK$  (H to J) 17978. Each experiment was independently replicated three times, and one representative data set was reported. (K) Quantification of fluorescent signal intensity in arbitrary intensity units (AIU,  $n = 300$ ). Error bars indicate standard deviations. An asterisk indicates significant differences relative to WT ( $P < 0.05$ ).

B). Both modifications are characteristic of increased LD-TPase activity, which is growth phase dependent in *E. coli* (41). We also found that relative to wild type, the  $\Delta mrcA$  strain generated 2-fold more 3-3 cross-links in logarithmic growth phase (Fig. 4A and Table S1A).

#### LD-TPases are essential for selection of colistin-resistant LOS<sup>-</sup> *A. baumannii*.

Next, we performed transposon sequencing in the  $\Delta mrcA$  mutant to determine genes that contribute to fitness relative to wild type. We discovered that two genes encoding putative LD-TPases (LdtJ and LdtK) were essential in the  $\Delta mrcA$  strain but not in wild type (Fig. 5A). As a control, we also show that mutations in *mrcB* were also synthetically lethal in *A. baumannii*, as previously reported in *E. coli* (42, 43). Since PBP1A inactivation supports colistin selection of LOS<sup>-</sup> *A. baumannii* (19), and mutations of *ldtJ* and *ldtK* are synthetically lethal in the  $\Delta mrcA$  strain, we hypothesized that LD-TPase activity could support viability of LOS<sup>-</sup> *A. baumannii*. LdtJ and LdtK both encode YkuD domains, which rely on essential cysteine residues to catalyze LD-TPase reactions (Fig. 5B). To test if LdtJ and LdtK contribute to selection of colistin-resistant LOS<sup>-</sup> *A. baumannii*, we engineered *ldtJ* and *ldtK* mutations in strain 19606, which produced LOS<sup>-</sup> isolates without compensatory *mrcA* mutations (18, 19). Colistin selection of each mutant failed to recover LOS<sup>-</sup> *A. baumannii* after multiple attempts (Fig. 5C and Table 1), showing each putative LD-TPase gene is required for LOS<sup>-</sup> viability. Complementation fully restored production of LOS<sup>-</sup> *A. baumannii* to wild-type levels. Furthermore, we also performed colistin selection experiments using *ldtJ* and *ldtK* mutants in strain Ab 5075. These data showed that Ab 5075 LD-TPase mutants were also unable to produce LOS<sup>-</sup> isolates relative to wild type (Fig. 5C and Table 1), which suggests a conserved role for LD-TPases in viability of LOS<sup>-</sup> *A. baumannii*.

To determine the LD-TPase activities of LdtJ and LdtK, the mutants were first treated with NADA and visualized.  $\Delta ldtJ$  (Fig. 5E) and  $\Delta ldtJ/pLdtJ_{C390}$  (Fig. 5F) strains showed a severe defect in NADA incorporation relative to wild type (Fig. 5D) and the mutant complemented with a wild-type allele (Fig. 5G), suggesting LdtJ is an LD-TPase that modifies peptidoglycan with D-amino acids.  $\Delta ldtK$  (Fig. 5H) and  $\Delta ldtK/pLdtK_{C138S}$  (Fig. 5I) strains showed a rounded cell morphology relative to wild type (Fig. 5D) and the complemented strain (Fig. 5J), suggesting a role for LdtK in elongation.

Fluorescence intensity (Fig. 5K) and cell shape (Fig. S6A) from NADA-treated cultures were quantified. The LD-TPase mutants were also defective in growth in Luria broth at 37°C relative to the wild-type and complemented strains (Fig. S6B).

#### **LdtJ forms 3-3 cross-links and incorporates D-amino acids into peptidoglycan.**

To define LD-TPase-dependent peptidoglycan modifications, we isolated peptidoglycan from strains 17978 (Table S1A) and 19606 (Table S1B). Muropeptides were generated by treatment with muramidase, separated by high-performance liquid chromatography, and if necessary, analyzed by tandem mass spectrometry (MS/MS) (Table S2) (19, 44). Peptidoglycan composition from the  $\Delta ldtJ$  mutant showed it was unable to generate 3-3 cross-links (Fig. 4A) or incorporate fluorescent D-amino acids along the lateral cell wall (Fig. 4B and Fig. 5E). The  $\Delta ldtJ$  strain also had reduced pools of muropeptides (Fig. 4C) with a concomitant increase in muretrapeptide abundance (Table S1A). Peptidoglycan isolated from stationary-phase  $\Delta ldtJ$  cells showed similar structures, where 3-3 cross-linking, fluorescent D-amino acid incorporation along the lateral cell wall, and muropeptide pools were significantly reduced relative to wild type (Fig. 4A to C). Similar trends were also found in 19606 (Table S1B). These studies indicate that LdtJ is an LD-TPase required for 3-3 cross-link formation in *A. baumannii*, while its presence also promotes LD-carboxypeptidase activity. While a previous report showed that D-Lys is incorporated into peptidoglycan of some strains of *A. baumannii* during stationary phase to protect the cell from effector proteins (44), here we showed via MS/MS that D-Asn, D-Arg, and D-Met are also incorporated into *A. baumannii* peptidoglycan via LdtJ activity in stationary phase (Fig. 4D and Table S1A and B).

**LdtK regulates outer membrane vesiculation.** In contrast to the  $\Delta ldtJ$  mutant, the muropeptide composition of the  $\Delta ldtK$  mutant showed slight increases of D-amino acid modification, 3-3 cross-linking, and muropeptide pools relative to wild type in logarithmic growth phase (Fig. 4A to D and Table S1A and B), indicating that LdtJ activity may increase in the absence of LdtK. We did not observe direct changes to LOS (Fig. S6C) or lipid A (Fig. S6D) structures in either the  $\Delta ldtJ$  or  $\Delta ldtK$  mutant. However, we found that the  $\Delta ldtK$  strain formed significantly more outer membrane vesicles (OMVs) than the wild type when total outer membrane vesicle protein content (Fig. 4E) or 3-deoxy-D-manno-oct-2-ulosonic acid (Kdo) concentrations (Fig. 4F) were quantified from outer membrane vesicles. In *E. coli*, LdtABC catalyzes transpeptidation between the outer membrane-anchored Braun's lipoprotein (Lpp) to peptidoglycan stem peptides, which stabilize the outer membrane lipid bilayer (30). We found that deletion of Lpp in *E. coli* resulted in hypervesiculation of the outer membrane, similar to  $\Delta ldtK$  *A. baumannii* (Fig. 4E and F). These studies suggest that LdtK functions to stabilize the outer membrane, possibly by linking it to other structures within the cell envelope. Interestingly, LOS<sup>-</sup> *A. baumannii* also produced significantly more outer membrane vesicles than wild type (Fig. 4E), suggesting the LOS-deficient outer membrane is unstable. Therefore, mechanisms that stabilize the outer membrane and cell envelope likely contribute to LOS<sup>-</sup> cell viability.

## **DISCUSSION**

The molecular factors that support *A. baumannii* survival without LOS are not well understood. LOS<sup>-</sup> *A. baumannii* assembles multiple septal sites to produce cell chains or filaments. A previous study found that PBP1A GTase activity inhibited isolation of colistin-resistant LOS<sup>-</sup> *A. baumannii* (19). Here, we showed that PBP1A GTase activity, which is presumably also required for its TPase activity, is required for proper cell division in *A. baumannii*. GTase inactivation resulted in septal site accumulation that correlated with selection of LOS<sup>-</sup> *A. baumannii*. *E. coli* cells are also known to form multiseptated chains upon LptC depletion or treatment with the LpxC inhibitor LPC-058, which compromise LPS transport and biosynthesis, respectively (29). Together, these studies support a model where septal defects support Gram-negative bacterial survival when LPS/LOS assembly and/or localization is compromised. Since we know outer membrane biogenesis limits the rate of LOS<sup>-</sup> *A. baumannii* growth (45), slowed septation via PBP1A mutation could reduce the growth rate enough to support LOS<sup>-</sup> outer

membrane biogenesis. Even more intriguing is the idea that increased formation of septal sites supports LOS<sup>-</sup> *A. baumannii* growth through outer membrane stabilization. In *E. coli*, transenvelope complexes with the Tol system and CpoB promote outer membrane constriction and septum peptidoglycan cleavage (23, 46, 47). While LPS/LOS is the major stabilizing factor in the outer membrane (13, 48), we do not understand how the lipid bilayer remains intact when LPS/LOS is compromised. However, increasing outer membrane attachment sites via septal site accumulation could increase LOS<sup>-</sup> outer membrane stability by directly linking it to other components within the cell envelope.

Cell division in *E. coli* is facilitated by the divisome complex, which includes more than 20 essential and accessory proteins that facilitate and regulate septal peptidoglycan synthesis, constrict the cell envelope, and separate the daughter cells. Divisome assembly is an ordered process where the Z-ring initially recruits class A PBPs via the FtsZ membrane anchors, FtsA-FtsN and ZipA, for a preseptal phase of peptidoglycan synthesis (49). Only after some delay, the next cell division proteins are recruited, including FtsQLB, FtsW-PBP3, and FtsN, which are required for constriction and daughter cell separation (50, 51). PBP1B associates with ZipA and FtsN (the latter interacts with FtsA) during the preseptal phase and later with FtsW/PBP3 and PBP3 (23, 24), and both its GTase and DD-TPase activities are stimulated by LpoB (46, 52, 53) and FtsN (54, 55).

Cell division in *A. baumannii* has not been well studied; however, we showed that the GTase activity of PBP1A promotes daughter cell separation. In *E. coli*, PBP1A localizes at the midcell in the absence of PBP1B, where it appears to compensate during division (26). Therefore, it is not unreasonable to suggest a primary role for PBP1A in septation in *A. baumannii*. Based on the formation of viable but chained *A. baumannii* in the *pbp1A* mutant, PBP1A GTase activity likely plays a role additional to FtsW-PBP3 in septal peptidoglycan synthesis. Since the PBP1A<sub>E92Q</sub> mutant forms a septum and constricts, but daughter cell separation is delayed, the GTase activity is likely required for the function of hydrolases, as shown in *E. coli* (56). Hence, PBP1A-mediated *de novo* peptidoglycan synthesis could be required for producing peptidoglycan that is remodeled by the hydrolases, which could couple peptidoglycan synthesis with daughter cell separation. Moreover, it appears as if GTase activity is required for PBP1A localization at the midcell in *A. baumannii*. PBP1A interaction with FtsW/PBP3 could be disrupted in the mutant, inhibiting septal localization. In *E. coli*, PBP1B GTase activity is regulated by many proteins (LpoA, FtsN, FtsW/PBP3, FtsQLB, and PgpB [57]), and so disruption of activity may result in mislocalization because it cannot associate with a specific regulatory factor. Further investigation is needed to understand if PBP1A directly contributes to septation via interactions with divisome components.

Since PBP1A inactivation supports colistin selection of LOS<sup>-</sup> *A. baumannii* (19), and *ldtJ* and *ldtK* are synthetically lethal in the  $\Delta mrcA$  mutant, each LD-TPase activity likely fortifies the cell envelope to support LOS<sup>-</sup> *A. baumannii* growth. Furthermore, the  $\Delta mrcA$  strain demonstrated a significant increase in 3-3 cross-linking relative to wild type (Fig. 4A). We showed that *LdtJ* is required for incorporation of D-amino acids, 3-3 cross-linking, and increased carboxypeptidase activity, while *LdtK* mutation decreased outer membrane stability. These distinct phenotypes indicate that separate LD-TPase activities coordinate to stabilize the cell envelope. *LdtJ* and *LdtK* have homology to *E. coli* *LdtD* and *LdtB*, respectively. *LdtD* works in complex with PBP1B and a D-alanyl-D-alanine carboxypeptidase (PBP6a) to increase the ratio of 3-3 to 4-3 cross-links, a mechanism that fortifies the cell envelope to enable *E. coli* survival when LPS transport is disrupted (29). *LdtB* catalyzes covalent linkage of outer membrane-anchored Braun's lipoprotein (Lpp) to peptidoglycan (32), while other Ldts covalently link outer membrane proteins to peptidoglycan (58, 59), which both presumably stabilize the cell envelope. Furthermore, our data indicate that *LdtJ* and *LdtK* could contribute comparable enzymatic activities in *A. baumannii*. Together, inactivation of PBP1A could support LOS<sup>-</sup> *A. baumannii* growth by inducing a septation defect, peptidoglycan remodeling, and cross-linking of outer membrane lipoprotein to peptidoglycan to collectively

stabilize the cell envelope when the major outer membrane-stabilizing factor, LPS/LOS, is compromised.

Intrinsic antimicrobial resistance is not well understood in *A. baumannii*, but our analysis indicates that PBP1A is an important component for  $\beta$ -lactam susceptibility. Our antimicrobial susceptibility studies suggest PBP1A<sup>DD</sup>-TPase activity contributes to 4-3 cross-links in both the Rod-complex and divisome, where the  $\Delta mrcA$  mutant showed increased susceptibility to Rod-complex- and divisome-targeting  $\beta$ -lactams. This is further supported by our PBP1A localization studies, where PBP1A is enriched at the midcell, where the divisome assembles, but also localizes along the lateral cell wall (Fig. 3), where the Rod-complex regulates peptidoglycan insertion to elongate rod-shaped bacteria. However, further studies are necessary to determine PBP1A contributions to both division and elongation in *A. baumannii*.

LD-TPases are targeted by carbapenems (38) and copper chloride (60), and we observed altered susceptibility to both in the *ldtJ* and *ldtK* mutants (Table 2). While we performed these studies in the single LD-TPase mutants, we were not able to engineer an *ldtJ ldtK* double mutant after several attempts, indicating that one of the genes may be required for *A. baumannii* survival. A more detailed analysis is needed to characterize the LdtJ and LdtK proteins to understand their contribution to resistance against clinically important antimicrobial compounds, which will inform more effective treatment strategies to combat *A. baumannii* infections.

## MATERIALS AND METHODS

**Bacterial strains and growth.** All strains and plasmids used in this study are listed in Table S3 in the supplemental material. All *A. baumannii* strains were grown from freezer stocks initially on Luria-Bertani (LB) agar at 37°C. For selection, 7.5  $\mu$ g/ml of kanamycin or 10  $\mu$ g/ml of colistin was used when appropriate. Strains that harbored the pABBRKn plasmid for complementation or overexpression were supplemented with 30  $\mu$ g/ml of kanamycin.

**Construction of PBP1A-mCherry fusions and overexpression vector.** Primers used in this study are listed in Table S4. The mCherry2B gene was amplified from pMV261 (61), purified, and cloned into the KpnI and SacI sites of pABBRKn (19) to generate pABBRKn::mCherry. The *mrcA* coding sequence (encoding PBP1A) from *A. baumannii* strain ATCC 17978 was amplified from plasmids pPBP1A, pPBP1A<sub>E92Q</sub>, and pPBP1A<sub>S459A</sub> (19); purified; and cloned into the XhoI and SacI sites in pABBRKn::mCherry, to create pPBP1A-mCherry, pPBP1A<sub>E92Q</sub>-mCherry, and pPBP1A<sub>S459A</sub>-mCherry, respectively. Plasmids were transformed into the  $\Delta mrcA$  mutant for localization studies.

To construct the inducible pPBP1A vector, the *mrcA* coding sequence (encoding PBP1A) was amplified from *A. baumannii* strain ATCC 17978 cDNA, digested with KpnI and Sall restriction enzymes, and cloned into pMMB67EHKn. The plasmid was transformed into the  $\Delta mrcA$  strain and induced with 2 mM isopropyl- $\beta$ -D-thiogalactopyranoside (IPTG) for overexpression studies.

**Construction of LD-transpeptidase genetic mutants.** All *A. baumannii* mutations were isolated as previously described (62). Briefly, REC<sub>ab</sub> (pAT03) was expressed in *A. baumannii* ATCC 17978 or 19606. A linear PCR product containing the FLP recombination target (FRT)-flanked kanamycin resistance cassette with flanking 125-bp regions of homology to either *ldtJ* or *ldtK* was transformed. Transformants were recovered in Luria broth, collected via centrifugation, and plated on LB supplemented with kanamycin. PCR and Sanger sequencing verified all genetic mutations.

Removal of the pMMB67EH::REC<sub>ab</sub> Tet<sup>r</sup> plasmid following isolation of mutants was performed as previously described (63). pMMB67EH carrying the FLP recombinase was transformed into cured mutants. Cells were recovered in Luria broth and plated on LB agar supplemented with IPTG to induce expression of the FLP recombinase. PCR was used to confirm excision of the kanamycin cassette.

For complementation, *ldtJ* or *ldtK* coding sequences were cloned into the XhoI and KpnI sites in pMMB67EHKn (19). Plasmids were transformed into the respective mutant to complement. For site-directed mutagenesis, complementation plasmids were amplified with primers to change the active-site cysteine residue to serine. Constructs were confirmed by Sanger sequencing and transformed into the respective mutant. *A. baumannii* mutants expressing complementation plasmids were grown in 2 mM IPTG to induce expression.

**Isolation of LOS<sup>-</sup> *A. baumannii* and determination of mutation frequency.** Isolation of LOS<sup>-</sup> *A. baumannii* colonies was done as previously described (19) with slight alterations. Briefly, cultures were grown to mid-logarithmic growth phase or stationary phase with or without antibiotics. One milliliter of optical density at 600 nm (OD<sub>600</sub>) of 1.0 (~10<sup>9</sup> CFU) was collected via centrifugation at 1,500  $\times$  *g*. Cells were washed with 1 ml of Luria broth and plated on LB agar supplemented with 10  $\mu$ g/ml of colistin. Isolated colonies were picked and replica plated on LB agar supplemented with vancomycin (10  $\mu$ g/ml) and LB agar supplemented with colistin (10  $\mu$ g/ml). Colonies sensitive to vancomycin but resistant to colistin were deemed LOS deficient.

Determination of the mutation frequency was done as previously described (19). The mutation frequency was calculated for three biological replicates, and one representative set was reported.



**Western blotting.** Western blot analysis was carried out via gel transfer to polyvinylidene difluoride (PVDF) (Thermo Fisher Scientific). All blots were blocked in 5% milk for 2 h. The primary antibodies anti-PBP1A ( $\alpha$ -PBP1A) and  $\alpha$ -NADH chain L were used at 1:1,000 and 1:500 (19), respectively, followed by  $\alpha$ -rabbit-horseradish peroxidase (HRP) secondary antibody at 1:10,000 (Thermo Fisher Scientific). SuperSignal West Pico Plus (Thermo Fisher Scientific) was used to measure relative protein concentrations.

**Peptidoglycan analysis.** Biological replicates were grown to either stationary or mid-logarithmic growth phase in 400 ml LB. Cells were collected at 4°C, suspended in 6 ml chilled 1 × phosphate-buffered saline (PBS), and lysed with dropwise addition to 6 ml boiling 8% SDS. Peptidoglycan was prepared from cell lysate as previously described (64). Briefly, muropeptides were released from peptidoglycan by the muramidase Cellosyl (Hoechst, Frankfurt am Main, Germany), reduced by sodium borohydride, and separated on a 250- by 4.6-mm 3- $\mu$ m Prontoasil 120-3-C<sub>18</sub> AQ reversed-phase column (Bischoff, Leonberg, Germany). The eluted muropeptides were detected by absorbance at 205 nm. Eluted peaks were assigned based on published chromatograms (19, 44); new peaks were subjected to MS/MS analysis. Peak means and variation from two independent biological repeats were reported for all samples.

**Fluorescent NADA staining.** Overnight cultures were back-diluted to an OD<sub>600</sub> of 0.05 and grown at 37°C in LB medium until they reached stationary or mid-logarithmic growth phase. Cells were washed once with Luria broth and resuspended in 1 ml Luria broth. Three microliters of 10 mM NBD-(linezolid-7-nitrobenz-2-oxa-1,3-diazol-4-yl)-amino-D-alanine (NADA) (Thermo Fisher) was added to the resuspension. Cells were incubated with NADA at 37°C for 30 min. Following incubation, cells were washed once and fixed with 1 × phosphate-buffered saline containing a (1:10) solution of 16% paraformaldehyde.

**Microscopy.** Fixed cells were immobilized on agarose pads and imaged using an inverted Nikon Eclipse Ti-2 widefield epifluorescence microscope equipped with a Photometrics Prime 95B camera and a Plan Apo 100× 1.45-numerical-aperture lens objective. Green fluorescence and red fluorescence images were taken using a filter cube with 470/40-nm or 560/40-nm excitation filters and 632/60 or 535/50 emission filters, respectively. Images were captured using NIS Elements software.

**Image analysis.** All microscopy images were processed and pseudocolored with ImageJ Fiji (65). A cyan lookup table was applied to NADA images, and a red lookup table was applied to mCherry images. The MicrobeJ plugin was used for quantifications (66). Cell lengths, widths, and fluorescence intensities as a function of length were quantified in MicrobeJ. Cell length, width, and fluorescence data were plotted in Prism 8 (GraphPad 8.4.1). NADA stain was pseudocolored using the MicrobeJ cyan lookup table. Phase and fluorescent channels were merged in MicrobeJ. Fluorescence localization graphs of dividing cells were generated using MicrobeJ XStatProfile. MicrobeJ feature detection was used to calculate the number of septal sites per cell stained with NADA as described above. Septal site percentages were represented with dot plots generated in Prism. Fifty cells were analyzed for fluorescent localization, and 300 cells were analyzed for all other experiments. Each experiment was independently replicated three times, one representative data set was reported in the quantification, and one representative image was included in the figure.

**Optical density growth curves.** Growth curves were performed as previously described (67). Briefly, overnight cultures were back-diluted to an OD<sub>600</sub> of 0.01 and set up as triplicate biological replicates in a 96-well plate (BrandTech Brand). A BioTek SynergyNeo<sup>2</sup> microplate reader was used to record optical density, which was read at OD<sub>600</sub> every half hour. The microplate reader was set to 37°C with continuous shaking. Growth curves were plotted in Prism 8. Each growth curve experiment was independently replicated three times, and one representative data set was reported.

**CFU growth curve.** Triplicate overnight cultures were diluted back to an OD<sub>600</sub> of 0.01 and grown for 12 h at 37°C in LB broth. Cells were plated at designated time points on LB agar. LB agar plates were grown overnight at 37°C, and the CFU were enumerated and reported. Growth curves were created in GraphPad Prism 8. Each growth curve experiment was independently replicated twice in triplicate, and one representative data set was reported. Doubling times were calculated using the exponential growth equation  $y(t) = y_0e^{kt}$  where  $y$  is cell density and  $k$  is growth rate. Standard deviation was calculated from the distribution among the reported data set.

**MIC calculation.** MIC assays were performed as previously described with slight modifications (48, 68). A small number of bacteria from an overnight plate were used to inoculate 5 ml LB at an OD<sub>600</sub> of 0.05 and grown to mid-logarithmic growth phase. Cells were washed twice with LB medium and diluted to an OD<sub>600</sub> of 0.01. One hundred fifty microliters of cells was added to each well of a 96-well plate. Antimicrobials and copper chloride (VWR) were diluted in water and serially diluted. Twofold dilutions of each compound were added to each well. Plates were incubated at 37°C overnight with shaking. MICs were determined by OD<sub>600</sub> measurements where cell density was 0. Each experiment was performed twice in triplicate, and a representative MIC was reported.

**Transposon sequencing.** Transposon sequencing was performed as previously described (69). Briefly, pJNW684 was conjugated into wild-type and  $\Delta mrcA$  *A. baumannii* strain ATCC 17978. A library of approximately 400,000 mutants was screened for growth in Luria broth. After 6 doublings, genomic DNA (gDNA) from cultures was isolated and sheared, and transposon junctions were amplified and sequenced. Transposon insertions from wild-type and  $\Delta mrcA$  strains were compared to determine factors that influence fitness. The transposon insertion maps for *ldtJ* and *ldtK* genes in wild-type and  $\Delta mrcA$  strains were reported.

**Outer membrane vesicle isolation.** Overnight cultures were back-diluted to an OD<sub>600</sub> of 0.01 and grown to stationary phase in 100 ml Luria broth as biological duplicates. Cultures were pelleted, and the supernatant was filtered through an 0.45- $\mu$ m filter (Fisherbrand). Equivalent volumes of filtered supernatant were subjected to ultracentrifugation (Sorvall WX 80+ ultracentrifuge with AH-629 swinging bucket



rotor) at 4°C for 1 h and  $151,243 \times g$ . The outer membrane vesicle pellet was resuspended in 500  $\mu$ l of cold buffer (50 mM Tris, 5 mM NaCl, 1 mM  $MgSO_4$ ; pH 7.5). Outer membrane vesicles from each strain were isolated three times in biological duplicates.

**Quantification of outer membrane vesicles.** For Bradford assays, a standard curve was prepared from dilution of bovine serum albumin (0 to 20 mg/ml) in Pierce Coomassie Plus assay reagent (ThermoFisher) to a final volume of 1 ml. In parallel, outer membrane vesicles (15, 20, and 30  $\mu$ l) were diluted in reagent to a final volume of 1 ml. Absorbance ( $OD_{595}$ ) was measured in a 96-well plate (BrandTech) using a microplate spectrophotometer (Fisherbrand AccuSkan). Optical densities of samples were compared to the standard curve plotted in Excel (Microsoft), and quantifications were graphed in Prism 8. Experiments were reproduced three times from each outer membrane vesicle isolation, and one representative data set was reported.

Kdo assays were performed as previously described (70). Briefly, 0 to 100  $\mu$ g/ml Kdo (Sigma) standards were diluted in parallel with isolated outer membrane vesicles (2, 5, 8, and 10  $\mu$ l) in 0.5 M  $H_2SO_4$  (Sigma). Outer membrane vesicle (OMV) isolates were boiled for 10 min. An 0.1 M concentration of periodic acid (Sigma), 0.2 M sodium arsenite (Sigma) in 0.5 M HCl (Sigma), and 0.6% thiobarbituric acid (Sigma) were incubated with Kdo standards and OMV isolates. All samples were boiled, and *n*-butanol (Sigma) was used to extract the purified Kdo prior to optical density measurements taken at  $OD_{552}$  and  $OD_{509}$  (Fisherbrand AccuSkan microplate spectrophotometer) in cuvettes (Fisherbrand). Readings at  $OD_{552}$  were subtracted from  $OD_{509}$  and used to generate a linear Kdo standard curve in Excel (Microsoft). Optical densities of samples were compared to the standard curve to quantify. Values were graphed in Prism 8. Each experiment was reproduced three times from each outer membrane vesicle isolation, and one representative data set was reported.

**Statistical analysis.** Tests for significance in differences of muropeptide composition and outer membrane vesicle production were conducted using the Student *t* test (two-tailed distribution with two-sample, equal variance calculations). Statistically significant differences between relevant strains possessed  $P < 0.05$ .

## SUPPLEMENTAL MATERIAL

Supplemental material is available online only.

**FIG S1**, TIF file, 1.6 MB.

**FIG S2**, TIF file, 1.8 MB.

**FIG S3**, TIF file, 2.5 MB.

**FIG S4**, TIF file, 1.1 MB.

**FIG S5**, TIF file, 1.5 MB.

**FIG S6**, TIF file, 0.9 MB.

**TABLE S1**, DOCX file, 0.03 MB.

**TABLE S2**, DOCX file, 0.01 MB.

**TABLE S3**, DOCX file, 0.03 MB.

**TABLE S4**, DOCX file, 0.01 MB.

## ACKNOWLEDGMENTS

This work was supported by funding from the National Institutes of Health (grant A1146829 to J.M.B., grant GM131317 to C.C.B.) and Research Councils UK (EP/T002778/1; to W.V.).

## REFERENCES

- Höltje JV. 1998. Growth of the stress-bearing and shape-maintaining murein sacculus of *Escherichia coli*. *Microbiol Mol Biol Rev* 62:181–203. <https://doi.org/10.1128/MMBR.62.1.181-203.1998>.
- Koch AL. 1988. Biophysics of bacterial walls viewed as stress-bearing fabric. *Microbiol Rev* 52:337–353. <https://doi.org/10.1128/MMBR.52.3.337-353.1988>.
- Rojas ER, Billings G, Odermatt PD, Auer GK, Zhu L, Miguel A, Chang F, Weibel DB, Theriot JA, Huang KC. 2018. The outer membrane is an essential load-bearing element in Gram-negative bacteria. *Nature* 559:617–621. <https://doi.org/10.1038/s41586-018-0344-3>.
- Raetz CRH, Whitfield C. 2002. Lipopolysaccharide endotoxins. *Annu Rev Biochem* 71:635–700. <https://doi.org/10.1146/annurev.biochem.71.110601.135414>.
- Zhou Z, White KA, Polissi A, Georgopoulos C, Raetz CR. 1998. Function of *Escherichia coli* MsbA, an essential ABC family transporter, in lipid A and phospholipid biosynthesis. *J Biol Chem* 273:12466–12475. <https://doi.org/10.1074/jbc.273.20.12466>.
- Polissi A, Georgopoulos C. 1996. Mutational analysis and properties of the *msbA* gene of *Escherichia coli*, coding for an essential ABC family transporter. *Mol Microbiol* 20:1221–1233. <https://doi.org/10.1111/j.1365-2958.1996.tb02642.x>.
- Braun M, Silhavy TJ. 2002. Imp/OstA is required for cell envelope biogenesis in *Escherichia coli*. *Mol Microbiol* 45:1289–1302. <https://doi.org/10.1046/j.1365-2958.2002.03091.x>.
- Ruiz N, Gronenberg LS, Kahne D, Silhavy TJ. 2008. Identification of two inner-membrane proteins required for the transport of lipopolysaccharide to the outer membrane of *Escherichia coli*. *Proc Natl Acad Sci U S A* 105:5537–5542. <https://doi.org/10.1073/pnas.0801196105>.
- Chng S-S, Gronenberg LS, Kahne D. 2010. Proteins required for lipopolysaccharide assembly in *Escherichia coli* form a transenvelope complex. *Biochemistry* 49:4565–4567. <https://doi.org/10.1021/bi100493e>.
- Sperandeo P, Cescutti R, Villa R, Benedetto CD, Candia D, Dehò G, Polissi A. 2007. Characterization of *lptA* and *lptB*, two essential genes implicated in lipopolysaccharide transport to the outer membrane of *Escherichia coli*. *J Bacteriol* 189:244–253. <https://doi.org/10.1128/JB.01126-06>.
- Sperandeo P, Lau FK, Carpentieri A, Castro CD, Molinaro A, Dehò G,

- Silhavy TJ, Polissi A. 2008. Functional analysis of the protein machinery required for transport of lipopolysaccharide to the outer membrane of *Escherichia coli*. *J Bacteriol* 190:4460–4469. <https://doi.org/10.1128/JB.00270-08>.
12. Wu T, McCandlish AC, Gronenberg LS, Chng S-S, Silhavy TJ, Kahne D. 2006. Identification of a protein complex that assembles lipopolysaccharide in the outer membrane of *Escherichia coli*. *Proc Natl Acad Sci U S A* 103:11754–11759. <https://doi.org/10.1073/pnas.0604744103>.
  13. Nikaido H. 2003. Molecular basis of bacterial outer membrane permeability revisited. *Microbiol Mol Biol Rev* 67:593–656. <https://doi.org/10.1128/mmr.67.4.593-656.2003>.
  14. Vaara M. 2010. Polymyxins and their novel derivatives. *Curr Opin Microbiol* 13:574–581. <https://doi.org/10.1016/j.mib.2010.09.002>.
  15. Cai Y, Chai D, Wang R, Liang B, Bai N. 2012. Colistin resistance of *Acinetobacter baumannii*: clinical reports, mechanisms and antimicrobial strategies. *J Antimicrob Chemother* 67:1607–1615. <https://doi.org/10.1093/jac/dks084>.
  16. Harris TL, Worthington RJ, Hittle LE, Zurawski DV, Ernst RK, Melander C. 2014. Small molecule downregulation of PmrAB reverses lipid A modification and breaks colistin resistance. *ACS Chem Biol* 9:122–127. <https://doi.org/10.1021/cb400490k>.
  17. Arroyo LA, Herrera CM, Fernandez L, Hankins JV, Trent MS, Hancock REW. 2011. The pmrCAB operon mediates polymyxin resistance in *Acinetobacter baumannii* ATCC 17978 and clinical isolates through phosphoethanolamine modification of lipid A. *Antimicrob Agents Chemother* 55:3743–3751. <https://doi.org/10.1128/AAC.00256-11>.
  18. Moffatt JH, Harper M, Harrison P, Hale JDF, Vinogradov E, Seemann T, Henry R, Crane B, St Michael F, Cox AD, Adler B, Nation RL, Li J, Boyce JD. 2010. Colistin resistance in *Acinetobacter baumannii* is mediated by complete loss of lipopolysaccharide production. *Antimicrob Agents Chemother* 54:4971–4977. <https://doi.org/10.1128/AAC.00834-10>.
  19. Boll JM, Crofts AA, Peters K, Cattoir V, Vollmer W, Davies BW, Trent MS. 2016. A penicillin-binding protein inhibits selection of colistin-resistant, lipooligosaccharide-deficient *Acinetobacter baumannii*. *Proc Natl Acad Sci U S A* 113:E6228–E6237. <https://doi.org/10.1073/pnas.1611594113>.
  20. Bertsche U, Breukink E, Kast T, Vollmer W. 2005. In vitro murein peptidoglycan synthesis by dimers of the bifunctional transglycosylase-transpeptidase PBP1B from *Escherichia coli*. *J Biol Chem* 280:38096–38101. <https://doi.org/10.1074/jbc.M508646200>.
  21. Cho H, Wivagg CN, Kapoor M, Barry Z, Rohs PDA, Suh H, Marto JA, Garner EC, Bernhardt TG. 2016. Bacterial cell wall biogenesis is mediated by SEDS and PBP polymerase families functioning semi-autonomously. *Nat Microbiol* 1:16172. <https://doi.org/10.1038/nmicrobiol.2016.172>.
  22. Vigouroux A, Cordier B, Aristov A, Alvarez L, Özbaykal G, Chaze T, Oldewurtel ER, Matondo M, Cava F, Bikard D, van Teeffelen S. 2020. Class-A penicillin binding proteins do not contribute to cell shape but repair cell-wall defects. *Elife* 9:e51998. <https://doi.org/10.7554/eLife.51998>.
  23. Gray AN, Egan AJ, van't Veer IL, Verheul J, Colavin A, Koumoutsi A, Biboy J, Altelaar AFM, Damen MJ, Huang KC, Simorre J-P, Breukink E, den Blaauwen T, Typas A, Gross CA, Vollmer W. 2015. Coordination of peptidoglycan synthesis and outer membrane constriction during *Escherichia coli* cell division. *Elife* 4:e07118. <https://doi.org/10.7554/eLife.07118>.
  24. Bertsche U, Kast T, Wolf B, Fraipont C, Aarsman MEG, Kannenber K, von Rechenberg M, Nguyen-Distèche M, den Blaauwen T, Höltje J-V, Vollmer W. 2006. Interaction between two murein (peptidoglycan) synthases, PBP3 and PBP1B, in *Escherichia coli*. *Mol Microbiol* 61:675–690. <https://doi.org/10.1111/j.1365-2958.2006.05280.x>.
  25. Du S, Lutkenhaus J. 2017. Assembly and activation of the *Escherichia coli* divisome. *Mol Microbiol* 105:177–187. <https://doi.org/10.1111/mmi.13696>.
  26. Banzhaf M, van den Berg van Saparoea B, Terrak M, Fraipont C, Egan A, Philippe J, Zapun A, Breukink E, Nguyen-Distèche M, den Blaauwen T, Vollmer W. 2012. Cooperativity of peptidoglycan synthases active in bacterial cell elongation. *Mol Microbiol* 85:179–194. <https://doi.org/10.1111/j.1365-2958.2012.08103.x>.
  27. Vollmer W, Blanot D, de Pedro MA. 2008. Peptidoglycan structure and architecture. *FEMS Microbiol Rev* 32:149–167. <https://doi.org/10.1111/j.1574-6976.2007.00094.x>.
  28. Vollmer W, Bertsche U. 2008. Murein (peptidoglycan) structure, architecture and biosynthesis in *Escherichia coli*. *Biochim Biophys Acta* 1778:1714–1734. <https://doi.org/10.1016/j.bbamem.2007.06.007>.
  29. Morè N, Martorana AM, Biboy J, Otten C, Winkle M, Serrano CKG, Montón Silva A, Atkinson L, Yau H, Breukink E, den Blaauwen T, Vollmer W, Polissi A. 2019. Peptidoglycan remodeling enables *Escherichia coli* to survive severe outer membrane assembly defect. *mBio* 10:e0279-18. <https://doi.org/10.1128/mBio.02729-18>.
  30. Magnet S, Dubost L, Marie A, Arthur M, Gutmann L. 2008. Identification of the L,D-transpeptidases for peptidoglycan cross-linking in *Escherichia coli*. *J Bacteriol* 190:4782–4785. <https://doi.org/10.1128/JB.00025-08>.
  31. Caveney NA, Caballero G, Voedts H, Niciforovic A, Worrall LJ, Vuckovic M, Fonvielle M, Hugonnet J-E, Arthur M, Strynadka NCJ. 2019. Structural insight into YcbB-mediated beta-lactam resistance in *Escherichia coli*. *Nat Commun* 10:1849. <https://doi.org/10.1038/s41467-019-09507-0>.
  32. Magnet S, Bellais S, Dubost L, Fourgeaud M, Mainardi J-L, Petit-Frère S, Marie A, Mengin-Lecreux D, Arthur M, Gutmann L. 2007. Identification of the L,D-transpeptidases responsible for attachment of the Braun lipoprotein to *Escherichia coli* peptidoglycan. *J Bacteriol* 189:3927–3931. <https://doi.org/10.1128/JB.00084-07>.
  33. Kuru E, Hughes HV, Brown PJ, Hall E, Tekkam S, Cava F, de Pedro MA, Brun YV, VanNieuwenhze MS. 2012. In situ probing of newly synthesized peptidoglycan in live bacteria with fluorescent D-amino acids. *Angew Chem Int Ed Engl* 51:12519–12523. <https://doi.org/10.1002/anie.201206749>.
  34. Kuru E, Lambert C, Rittichier J, Till R, Ducret A, Derouaux A, Gray J, Biboy J, Vollmer W, VanNieuwenhze M, Brun YV, Sockett RE. 2017. Fluorescent D-amino-acids reveal bi-cellular cell wall modifications important for *Bdellovibrio bacteriovorus* predation. *Nat Microbiol* 2:1648–1657. <https://doi.org/10.1038/s41564-017-0029-y>.
  35. Kuru E, Radkov A, Meng X, Egan A, Alvarez L, Dowson A, Booher G, Breukink E, Roper DI, Cava F, Vollmer W, Brun Y, VanNieuwenhze MS. 2019. Mechanisms of incorporation for D-amino acid probes that target peptidoglycan biosynthesis. *ACS Chem Biol* 14:2745–2756. <https://doi.org/10.1021/acscchembio.9b00664>.
  36. Baranowski C, Welsh MA, Sham L-T, Eskandarian HA, Lim HC, Kieser KJ, Wagner JC, McKinney JD, Fantner GE, Ioerger TR, Walker S, Bernhardt TG, Rubin EJ, Rego EH. 2018. Maturing *Mycobacterium smegmatis* peptidoglycan requires non-canonical crosslinks to maintain shape. *Elife* 7:e37516. <https://doi.org/10.7554/eLife.37516>.
  37. García-Heredia A, Pohane AA, Melzer ES, Carr CR, Fiolek TJ, Rundell SR, Lim HC, Wagner JC, Morita YS, Swarts BM, Siegrist MS. 2018. Peptidoglycan precursor synthesis along the sidewall of pole-growing mycobacteria. *Elife* 7:e37243. <https://doi.org/10.7554/eLife.37243>.
  38. Mainardi J-L, Hugonnet J-E, Rusconi F, Fourgeaud M, Dubost L, Mouton AN, Delfosse V, Mayer C, Gutmann L, Rice LB, Arthur M. 2007. Unexpected inhibition of peptidoglycan LD-transpeptidase from *Enterococcus faecium* by the beta-lactam imipenem. *J Biol Chem* 282:30414–30422. <https://doi.org/10.1074/jbc.M704286200>.
  39. Yourassowsky E, Linden MPVD, Lismont MJ, Crokaert F. 1989. Growth curve patterns of *Escherichia coli*, *Serratia marcescens*, and *Proteus vulgaris* submitted to different tigenom concentrations. *J Chemother* 1:49–53. <https://doi.org/10.1080/1120009X.1989.11738949>.
  40. Buijs J, Dofferhoff ASM, Mouton JW, Wagenvoort JHT, van der Meer JWM. 2008. Concentration-dependency of beta-lactam-induced filament formation in Gram-negative bacteria. *Clin Microbiol Infect* 14:344–349. <https://doi.org/10.1111/j.1469-0691.2007.01940.x>.
  41. Asmar AT, Ferreira JL, Cohen EJ, Cho S-H, Beeby M, Hughes KT, Collet J-F. 2017. Communication across the bacterial cell envelope depends on the size of the periplasm. *PLoS Biol* 15:e2004303. <https://doi.org/10.1371/journal.pbio.2004303>.
  42. Paradis-Bleau C, Markovski M, Uehara T, Lupoli TJ, Walker S, Kahne DE, Bernhardt TG. 2010. Lipoprotein cofactors located in the outer membrane activate bacterial cell wall polymerases. *Cell* 143:1110–1120. <https://doi.org/10.1016/j.cell.2010.11.037>.
  43. Typas A, Banzhaf M, Gross CA, Vollmer W. 2011. From the regulation of peptidoglycan synthesis to bacterial growth and morphology. *Nat Rev Microbiol* 10:123–136. <https://doi.org/10.1038/nrmicro2677>.
  44. Le N-H, Peters K, Espaillet A, Sheldon JR, Gray J, Venanzio GD, Lopez J, Djahanschiri B, Mueller EA, Hennon SW, Levin PA, Ebersberger I, Skaar EP, Cava F, Vollmer W, Feldman MF. 2020. Peptidoglycan editing provides immunity to *Acinetobacter baumannii* during bacterial warfare. *Sci Adv* 6:eabb5614. <https://doi.org/10.1126/sciadv.abb5614>.
  45. Nagy E, Losick R, Kahne D. 2019. Robust suppression of lipopolysaccharide deficiency in *Acinetobacter baumannii* by growth in minimal medium. *J Bacteriol* 201:e00420-19. <https://doi.org/10.1128/JB.00420-19>.
  46. Egan AJF, Maya-Martinez R, Ayala I, Bougault CM, Banzhaf M, Breukink E, Vollmer W, Simorre J-P. 2018. Induced conformational changes activate the peptidoglycan synthase PBP1B. *Mol Microbiol* 110:335–356. <https://doi.org/10.1111/mmi.14082>.
  47. Yakhnina AA, Bernhardt TG. 2020. The Tol-Pal system is required for

- peptidoglycan-cleaving enzymes to complete bacterial cell division. *Proc Natl Acad Sci U S A* 117:6777–6783. <https://doi.org/10.1073/pnas.1919267117>.
48. Kang KN, Klein DR, Kazi MI, Guérin F, Cattoir V, Brodbelt JS, Boll JM. 2019. Colistin heteroresistance in *Enterobacter cloacae* is regulated by PhoQ-dependent 4-amino-4-deoxy-l-arabinose addition to lipid A. *Mol Microbiol* 111:1604–1616. <https://doi.org/10.1111/mmi.14240>.
  49. Pazos M, Peters K, Casanova M, Palacios P, VanNieuwenhze M, Breukink E, Vicente M, Vollmer W. 2018. Z-ring membrane anchors associate with cell wall synthases to initiate bacterial cell division. *Nat Commun* 9:5090. <https://doi.org/10.1038/s41467-018-07559-2>.
  50. Haeusser DP, Margolin W. 2016. Splitsville: structural and functional insights into the dynamic bacterial Z ring. *Nat Rev Microbiol* 14:305–319. <https://doi.org/10.1038/nrmicro.2016.26>.
  51. Aarsman MEG, Piette A, Fraipont C, Vinkenvleugel TMF, Nguyen-Distèche M, den Blaauwen T. 2005. Maturation of the *Escherichia coli* divisome occurs in two steps. *Mol Microbiol* 55:1631–1645. <https://doi.org/10.1111/j.1365-2958.2005.04502.x>.
  52. Typas A, Banzhaf M, van den Berg van Saparoea B, Verheul J, Biboy J, Nichols RJ, Zietek M, Beilharz K, Kannenberg K, von Rechenberg M, Breukink E, den Blaauwen T, Gross CA, Vollmer W. 2010. Regulation of peptidoglycan synthesis by outer-membrane proteins. *Cell* 143:1097–1109. <https://doi.org/10.1016/j.cell.2010.11.038>.
  53. Egan AJF, Jean NL, Koumoutsi A, Bougault CM, Biboy J, Sassine J, Solovyova AS, Breukink E, Typas A, Vollmer W, Simorre J-P. 2014. Outer-membrane lipoprotein LpoB spans the periplasm to stimulate the peptidoglycan synthase PBP1B. *Proc Natl Acad Sci U S A* 111:8197–8202. <https://doi.org/10.1073/pnas.1400376111>.
  54. Müller P, Ewers C, Bertsche U, Anstett M, Kallis T, Breukink E, Fraipont C, Terrak M, Nguyen-Distèche M, Vollmer W. 2007. The essential cell division protein FtsN interacts with the murein (peptidoglycan) synthase PBP1B in *Escherichia coli*. *J Biol Chem* 282:36394–36402. <https://doi.org/10.1074/jbc.M706390200>.
  55. Egan AJF, Biboy J, van't Veer I, Breukink E, Vollmer W. 2015. Activities and regulation of peptidoglycan synthases. *Philos Trans R Soc Lond B Biol Sci* 370:20150031. <https://doi.org/10.1098/rstb.2015.0031>.
  56. Banzhaf M, Yau HC, Verheul J, Lodge A, Kritikos G, Mateus A, Cordier B, Hov AK, Stein F, Wartel M, Pazos M, Solovyova AS, Breukink E, van Teeffelen S, Savitski MM, den Blaauwen T, Typas A, Vollmer W. 2020. Outer membrane lipoprotein Nlpl scaffolds peptidoglycan hydrolases within multi-enzyme complexes in *Escherichia coli*. *EMBO J* 39:e102246. <https://doi.org/10.15252/embj.2019102246>.
  57. Hernández-Rocamora VM, Otten CF, Radkov A, Simorre J-P, Breukink E, VanNieuwenhze M, Vollmer W. 2018. Coupling of polymerase and carrier lipid phosphatase prevents product inhibition in peptidoglycan synthesis. *Cell Surf* 2:1–13. <https://doi.org/10.1016/j.tscw.2018.04.002>.
  58. Sandoz KM, Moore RA, Beare PA, Patel AV, Smith RE, Bern M, Hwang H, Cooper CJ, Priola SA, Parks JM, Gumbart JC, Mesnage S, Heinzen RA. 2020.  $\beta$ -Barrel proteins tether the outer membrane in many Gram-negative bacteria. *Nat Microbiol* <https://doi.org/10.1038/s41564-020-00798-4>.
  59. Godessart P, Lannoy A, Dieu M, Van der Verren SE, Soumillion P, Collet J-F, Remaut H, Renard P, De Bolle X. 2020.  $\beta$ -Barrels covalently link peptidoglycan and the outer membrane in the  $\alpha$ -proteobacterium *Brucella abortus*. *Nat Microbiol* <https://doi.org/10.1038/s41564-020-00799-3>.
  60. Peters K, Pazos M, Edoó Z, Hugonnet J-E, Martorana AM, Polissi A, VanNieuwenhze MS, Arthur M, Vollmer W. 2018. Copper inhibits peptidoglycan LD-transpeptidases suppressing  $\beta$ -lactam resistance due to bypass of penicillin-binding proteins. *Proc Natl Acad Sci U S A* 115:10786–10791. <https://doi.org/10.1073/pnas.1809285115>.
  61. Stover CK, de la Cruz VF, Fuerst TR, Burlein JE, Benson LA, Bennett LT, Bansal GP, Young JF, Lee MH, Hatfull GF. 1991. New use of BCG for recombinant vaccines. *Nature* 351:456–460. <https://doi.org/10.1038/351456a0>.
  62. Tucker AT, Nowicki EM, Boll JM, Knauf GA, Burdis NC, Trent MS, Davies BW. 2014. Defining gene-phenotype relationships in *Acinetobacter baumannii* through one-step chromosomal gene inactivation. *mBio* 5:e01313-14. <https://doi.org/10.1128/mBio.01313-14>.
  63. Boll JM, Tucker AT, Klein DR, Beltran AM, Brodbelt JS, Davies BW, Trent MS. 2015. Reinforcing lipid A acylation on the cell surface of *Acinetobacter baumannii* promotes cationic antimicrobial peptide resistance and desiccation survival. *mBio* 6:e00478-15. <https://doi.org/10.1128/mBio.00478-15>.
  64. Glauner B, Höltje JV, Schwarz U. 1988. The composition of the murein of *Escherichia coli*. *J Biol Chem* 263:10088–10095.
  65. Schindelin J, Arganda-Carreras I, Frise E, Kaynig V, Longair M, Pietzsch T, Preibisch S, Rueden C, Saalfeld S, Schmid B, Tinevez J-Y, White DJ, Hartenstein V, Eliceiri K, Tomancak P, Cardona A. 2012. Fiji: an open-source platform for biological-image analysis. *Nat Methods* 9:676–682. <https://doi.org/10.1038/nmeth.2019>.
  66. Ducret A, Quardokus EM, Brun YV. 2016. MicrobeJ, a tool for high throughput bacterial cell detection and quantitative analysis. *Nat Microbiol* 1:16077. <https://doi.org/10.1038/nmicrobiol.2016.77>.
  67. Kazi MI, Perry BW, Card DC, Schargel RD, Ali HB, Obuekwe VC, Sapkota M, Kang KN, Pellegrino MW, Greenberg DE, Castoe TA, Boll JM. 2020. Discovery and characterization of New Delhi metallo- $\beta$ -lactamase-1 inhibitor peptides that potentiate meropenem-dependent killing of carbapenemase-producing Enterobacteriaceae. *J Antimicrob Chemother* 75:2843–2851. <https://doi.org/10.1093/jac/dkaa242>.
  68. Guérin F, Isnard C, Sinel C, Morand P, Dhalluin A, Cattoir V, Giard J-C. 2016. Cluster-dependent colistin hetero-resistance in *Enterobacter cloacae* complex. *J Antimicrob Chemother* 71:3058–3061. <https://doi.org/10.1093/jac/dkw260>.
  69. Kazi MI, Schargel RD, Boll JM. 2020. Generating transposon insertion libraries in Gram-negative bacteria for high-throughput sequencing. *J Vis Exp* (161):e61612. <https://doi.org/10.3791/61612>.
  70. Marolda CL, Lahiry P, Vinés E, Saldías S, Valvano MA. 2006. Micromethods for the characterization of lipid A-core and O-antigen lipopolysaccharide. *Methods Mol Biol* 347:237–252. <https://doi.org/10.1385/1-59745-167-3:237>.